

Charge fluctuations across the pressure-induced quantum phase transition in $\text{EuCu}_2(\text{Ge}_{1-x}\text{Si}_x)_2$

Mahmoud A. Ahmida,^{1,*} Martin K. Forthaus,¹ Christoph Geibel,² Zakir Hossain,³ Giovanni R. Hearne,⁴ Jirka Kaštil,⁵ Jiri Prchal,⁶ Vladimír Sechovský,⁶ and Mohsen M. Abd-Elmeguid^{1,†}

¹*II. Physikalisches Institut, Universität zu Köln, Zùlpicher Str. 77, 50937 Köln, Germany*

²*Max-Planck-Institute for Chemical Physics of Solids, Nöthnitzer Str. 40, 01187 Dresden, Germany*

³*Department of Physics, Indian Institute of Technology, Kanpur 208016, India*

⁴*Department of Physics, University of Johannesburg, PO Box 524, Auckland Park, 2006, Johannesburg, South Africa*

⁵*Institute of Physics, Academy of Sciences of the Czech Republic, Na Slovance 1999/2, Prague 8, Czech Republic*

⁶*Department of Condensed Matter Physics, Faculty of Mathematics and Physics, Charles University, Ke Karlovu 5, Prague 2, Czech Republic*



(Received 6 March 2020; revised manuscript received 23 April 2020; accepted 23 April 2020; published 18 May 2020)

Pressurizing strategically selected compositions of the $\text{EuCu}_2(\text{Ge}_{1-x}\text{Si}_x)_2$ series affords an opportunity for gaining microscopic insight into the ground-state properties and interplay between magnetism and valence fluctuations across a quantum critical point. This is investigated by way of systematic ^{151}Eu Mössbauer spectroscopy measurements on $x = 0$ and $x = 0.5$ compositions in the series, pressurized up to 7 GPa including variable temperature scans in the range 300–4.2 K. In EuCu_2Ge_2 the temperature and pressure dependences of the hyperfine interaction parameters indicate that both the magnetic and divalent state, $\text{Eu}^{\nu+}$ where $\nu = 2$, are stable up to 6–7 GPa, thus serving as a useful reference. Whereas in the $x = 0.5$ composition which initially involves Eu^{2+} , collapse of the magnetically ordered state is onset at ~ 1.3 GPa and there is emergence of a nonmagnetic intermediate valence state coexisting with the magnetically ordered state. This regime of mixed states is a precursor of a quantum phase transition to a nonmagnetic homogeneous intermediate valence state $\nu \sim 2.45$, across a quantum critical point at 3.6 GPa, suggesting a first-order phase transition. X-ray-diffraction pressure studies at 300 K up to 6 GPa of the $x = 0.5$ composition indicate there is no change in lattice symmetry from the tetragonal ThCr_2Si_2 -type structure. There are also no obvious discontinuities in pressure dependences of the lattice parameters upon evolving through the quantum critical point at 3.6 GPa. Increasing pressure changes the starting Eu^{2+} valence monotonically, until the mean valence attains its largest value $\nu \sim 2.45$ indicative of enhanced charge fluctuations at the quantum critical point and plateaus thereafter. High-pressure resistance measurements at low temperatures down to 40 mK near the quantum critical point reveal no evidence for superconductivity.

DOI: [10.1103/PhysRevB.101.205127](https://doi.org/10.1103/PhysRevB.101.205127)

I. INTRODUCTION

In recent years the investigation of magnetically ordered $4f$ electron systems near or at a quantum phase transition (QPT) has attracted considerable interest. This is due to the fact that QPTs are driven by a corresponding change of quantum fluctuations between phases across a quantum critical point (QCP). These fluctuations strongly affect the physical properties of the system at finite temperatures in the vicinity of a QCP [1], resulting in the formation of unusual ground states including unconventional superconductivity [2–4]. Most of the investigated systems have been Ce-based compounds which exhibit magnetic quantum critical points either by doping or by applying external pressure. Well-known examples involving pressure tuning through a QCP are $\text{CeCu}_{6-x}\text{Au}_6$ [5], CePd_2Si_2 [6], and CeIn_3 [7], which undergo a second-order

magnetic to nonmagnetic transition through a QCP. In the case of CePd_2Si_2 and CeIn_3 superconductivity appears near the magnetic QCP. In this context, the observation of a distinct superconducting phase in CeCu_2Si_2 under high pressure ($T_C \sim 2$ K, $P \sim 4$ GPa) well beyond the superconducting phase at ambient pressure ($T_C = 0.7$ K) has generated considerable excitement [8,9]. While the superconducting phase at ambient pressure is believed to be due to critical spin fluctuations, the second one at higher pressure is suggested to be mediated by critical valence fluctuations near a second QCP [8,9].

There is also a more recent discovery in divalent antiferromagnetically ordered Eu metal under high pressure, where superconductivity emerges when pressure destabilizes the magnetic state [10,11]. In view of these findings in CeCu_2Si_2 and Eu metal, the investigation of valence fluctuations at or near a QCP is of fundamental interest to understand the nature of related unconventional ground states in this class of materials.

In this respect, the intermetallic $\text{EuCu}_2(\text{Ge}_{1-x}\text{Si}_x)_2$ series crystallizing in the tetragonal ThCr_2Si_2 -type structure is of particular interest. Progressing through this series combines

*Present address: Electrical Engineering Department, The Higher Institute of Sciences and Technology, Ajdabiya, Libya.

†Corresponding author: meguid@ph2.uni-koeln.de

the divalent Eu antiferromagnetic (AF) compound EuCu_2Ge_2 ($T_N = 14$ K) [12–14], with the nonmagnetic intermediate valence (IV) compound EuCu_2Si_2 [15]. Thus this offers the possibility to study the crossover from the magnetic to nonmagnetic IV state through a QCP. Structural, magnetic, and transport properties of the series have been extensively studied at ambient pressure [16–19]. The magnetic phase diagram of $\text{EuCu}_2(\text{Ge}_{1-x}\text{Si}_x)_2$ has been shown to be consistent with the Doniach phase diagram [20]. The AF phase is stable up to $x \leq 0.6$ and disappears abruptly for $x > 0.65$, while the lattice structure remains unchanged. Here T_N first increases with increasing Si concentration, passes through a maximum $T_N = 20$ K at $x = 0.50$, and sharply decreases, indicating a magnetic QCP close to $x \sim 0.70$. Near the QCP heavy quasiparticles have been found at low temperatures [16,17].

An alternative approach to such composition-varying studies is to investigate the QPT in $\text{EuCu}_2(\text{Ge}_{1-x}\text{Si}_x)_2$ induced by external pressure at fixed Si concentrations. This is due to the fact that the ionic radius of the Eu^{3+} ($J = 0$) nonmagnetic state is smaller than that of the Eu^{2+} ($J = 7/2$) magnetically ordered state. Thus, external pressure can be used to generate well-defined incremental changes of the relevant magnetic-electronic properties of the system and thereby drive the system from the stable Eu^{2+} AF state to a nonmagnetic IV or Eu^{3+} state across a quantum phase transition. This has the advantage of being able to tune physical properties for a fixed composition without affecting the band structure.

Indeed, very recently Iha *et al.* [21] reported on the evolution of the electronic and magnetic properties of single crystals of $\text{EuCu}_2(\text{Ge}_{1-x}\text{Si}_x)_2$ with $x = 0, 0.45$, and 0.6 under external pressure using macroscopic (susceptibility and resistivity) experimental probes. The results basically revealed similar behavior of the electronic and magnetic properties with increasing pressure and Si concentrations [16]. These studies indicate collapse of AF ordering at a QCP corresponding to a critical pressure P_C of ~ 7 GPa and ~ 4 GPa for the $x = 0$ and 0.45 compositions, respectively, suggested to be associated with a change of valence from Eu^{2+} towards an IV or Eu^{3+} state [21]. However, such macroscopic methods do not allow accurate determination of the possible valence changes across the QCP.

Moreover, it should be noted that Iha *et al.* [21] and more recently the photoemission studies of Kawasaki *et al.* [22] clearly show that at ambient pressure EuCu_2Ge_2 is in a stable Eu^{2+} state, consistent with previous reports [12–14]. This contrasts with what is reported in x-ray absorption near-edge spectroscopy (XANES) studies [19,23,24], where EuCu_2Ge_2 is suggested to be in an IV state already at ambient pressure.

Thus, the valence at ambient pressure and evolution of the valence and magnetic states with pressure across the QCP of $\text{EuCu}_2(\text{Ge}_{1-x}\text{Si}_x)_2$ merits further investigation. To this end in the present work we have investigated the pressure-induced change of valence and magnetic states on a *microscopic level* across the QCP of $\text{EuCu}_2(\text{Ge}_{1-x}\text{Si}_x)_2$. The technique of choice for this purpose is ^{151}Eu Mössbauer effect (ME) spectroscopy, here extended up to 7 GPa and coupled to variable temperature measurements in the range 300–4.2 K. This is considered a powerful technique for directly and simultaneously monitoring pressure-induced changes of both Eu valence (via the isomer shift S) and ordered magnetic

state of the Eu ions (via the effective magnetic hyperfine field B_{eff} at the Eu nucleus). In particular, the isomer shift is very sensitive to the valence state of Eu, as the $\text{Eu}^{3+}-4f^6$ configuration allows a higher s -electron density at the Eu nucleus than $\text{Eu}^{2+}-4f^7$. This results in a difference of isomer shift values between $\text{Eu}^{2+}(S_2)$ and $\text{Eu}^{3+}(S_3)$ of $\Delta S = |S_3 - S_2|$ in the range 10–13 mm/s, considerably larger than the resolution-limiting experimental resonance linewidth (~ 2.5 mm/s).

Moreover, the $\sim 10^{-8}$ s probing time of the ^{151}Eu ME technique is much longer than typical $\sim 10^{-13}$ s valence fluctuation times that may occur between two electronic configurations of Eu in metallic systems [25]. In such cases ^{151}Eu ME conspicuously detects a mean valence $\text{Eu}^{\nu+}$ with $2 < \nu < 3$, i.e., an IV state. The benefits of employing ^{151}Eu ME for this purpose under extreme pressure-temperature conditions are exemplified in Sec. III B.

For an accurate determination of the Eu valence state and as the unit cell of the $\text{EuCu}_2(\text{Ge}_{1-x}\text{Si}_x)_2$ series decreases with increasing Si concentration, two different antiferromagnetically ordered compositions have been selected for pressurization, namely, $x = 0.5$ close to the QCP composition $x \sim 0.7$ and for comparison the undoped end member EuCu_2Ge_2 ($x = 0$) which is far away from the QCP.

Our ^{151}Eu ME studies at variable low temperatures reveal that in EuCu_2Ge_2 both the magnetic and valence states are stable up to ~ 6 GPa, whereas the sample with $x = 0.5$, initially involving the Eu^{2+} valence, undergoes a collapse of magnetic ordering in the range 2.2–3.6 GPa associated with a large shift of the Eu mean valence towards an IV state. A pressure-induced QPT is found at a critical pressure $P_C \sim 3.6$ GPa, while the lattice structure remains stable through this pressure regime. Enhanced valence fluctuations $\nu \sim 2.5$ are discerned at the QCP, but no evidence for superconductivity is observed at low temperatures down to 40 mK. The results render a magnetic-electronic phase diagram demonstrating the interplay between magnetic ground state and valence state across the pressure-induced QPT in $\text{EuCu}_2(\text{Ge}_{0.5}\text{Si}_{0.5})_2$.

II. EXPERIMENT

Samples involving the two compositions $x = 0$ and $x = 0.5$ in the series $\text{EuCu}_2(\text{Ge}_{1-x}\text{Si}_x)_2$ were derived from the same well-characterized batches of Ref. [16], in which single-phase materials were obtained.

A. ^{151}Eu Mössbauer spectroscopy: high-pressure methodology

A high-pressure cell of the Chester-Jones type was used for compressing comparatively large sample volumes up to several GPa in the cavity of a confining gasket sandwiched between opposing boron carbide (B_4C) anvils with culets of 6-mm diameter [26,27]. For ^{151}Eu Mössbauer spectroscopy these anvils permit sufficient transmission of the 21.6-keV resonance radiation derived from a 100-mCi source of ^{151}Sm F_3 with an active diameter of 6 mm. Source on a transducer and sample (absorber) in the pressure cell were configured on a probe in a vertical transmission geometry and top loaded into a cryostat for measurements in the range 300–4.2 K. Source and absorber were normally at the same temperature. A Ge

detector was used to detect the radiation transmitted through the Mylar windows of the cryostat.

Absorbers were in the form of epoxy-cast pellets (diameter 3.5 mm and initial thickness 0.5 mm) loaded into the 4-mm-diameter cavity drilled into appropriately hardened Cu-Be gaskets preindented to a thickness of 0.6 mm prior to loading the sample pellet. This as-cast sample pellet arrangement ensured a homogeneous mixture and quasihydrostatic medium for the grains when the absorber was under high pressure. Optimal sample thicknesses of ~ 2.9 mg/cm² were calculated. This takes into account electronic absorption of the 21.6-keV resonance radiation by the constituent elements in the sample compositions and also ensures an optimal thickness of resonance atoms for an adequate resonance effect in acceptable data acquisition durations of ~ 24 h. To this end ~ 15 mg of EuCu₂Ge₂ and EuCu₂(Si_{0.5}Ge_{0.5})₂ compositions were used as a fine powder in the above-mentioned epoxy-cast pellets.

A Ge sensor for temperature measurements was lodged in a slot in the pressure cell at 10-mm proximity to the sample. A manganin wire wound resistance of 50 Ω was wrapped around the bottom region of the of the pressure cell for heating purposes.

In situ pressures were obtained by measuring T_C of a superconducting lead manometer in the sample cavity [28]. The broadening of the transition was used to ascertain the pressure gradient in the pressurized cavity. A thin high-purity (99.999%) lead strip was glued on a Mylar foil of 3.5-mm diameter and 1.0-mm thickness. This manometer disk was placed directly on the sample disk. Kapton foil of 40- μ m thickness was fixed on the CuBe gasket to insulate the 70- μ m diameter Cu wires used to make the four-probe contacts to the lead strip. Outside of the CuBe gasket area thicker Cu leads were used to convey the excitation current and sensed voltage signals between the four-probe contacts on the lead manometer and the current source and voltmeter.

The Mössbauer spectra were analyzed with the NORMOS software package [29], to derive the pertinent hyperfine interaction parameters, isomer shift S , magnetic hyperfine field B_{eff} , and absorption areas (abundances) of spectral components.

B. X-ray-diffraction measurements under pressure

Energy-dispersive x-ray-diffraction (ED-XRD) measurements were performed at the beamline F2.1, HASYLAB, using the MAX80 multianvil-type x-ray system in which six tungsten carbide anvils compress a sample volume configured in a cube capsule [30]. Powdered sample is loaded into the cylindrical recess in the boron-epoxy capsule cube of edge length 6 mm. In the recess the sample is confined in the 1-mm inner diameter of a BN cylinder closed with compressed BN powder caps. This acts as a confining cavity and pressure-transmitting medium. As a pressure marker NaCl powder is also loaded into the cylindrical recess of the capsule. Pressure is generated by a 250-ton hydraulic ram and the maximum attainable pressure is mainly determined by the 6-mm edge length of the tungsten carbide anvil face. Pressures up to ~ 7 GPa were obtained by applying 50 tons of force to the tungsten carbide anvils. The synchrotron beam was guided

between the tungsten anvils through the sample. A Ge detector was mounted at a fixed 2θ angle with respect to the incident beam such that

$$E d_{hkl} = \frac{hc}{2 \sin \theta} = \frac{6.199}{\sin \theta} \text{ keV \AA} = 72.933 \text{ keV \AA}, \quad (1)$$

for the reflection at energy E satisfying Bragg's law for the d_{hkl} plane.

At each pressure an ED-XRD spectrum was recorded for both the sample and the NaCl pressure calibrant. The spectra were analyzed using the program EDXPOWD 3.13 which was specially developed by F. Porsch (RTI GmbH Paderborn, Germany, 1996) for high-pressure x-ray diffraction using the diamond-anvil cell. The Decker equation of state was used to determine the pressure from the derived lattice parameter of the NaCl [31].

C. High-pressure resistance-temperature measurements

Resistance-temperature scans of EuCu₂(Ge_{1-x}Si_x)₂ with $x = 0.5$ were measured under hydrostatic pressure up to 3 GPa and at low temperatures down to 40 mK using a double-wall piston-cylinder pressure cell [32]. Daphne 7373 oil was used as a pressure-transmitting medium [33,34]. The pressure was determined by a manganin wire resistance at room temperature and corrected for low temperatures. Electrical resistance measurements were performed by a standard four-wire technique with lock-in detection in the temperature range 300–2 K using the electrical transport option of the physical properties measurement system of Quantum Design. A dilution refrigerator was used to measure resistances down to 40 mK in the case of the highest pressure attained of ~ 3 GPa. The resistance-temperature measurements and search for superconductivity near a QCP [35] may be compared with that of Iha *et al.* [21] on the $x = 0.45$ composition.

III. RESULTS AND DISCUSSION

We present and discuss the change of the structural, electronic, and magnetic properties of EuCu₂Ge₂ and EuCu₂(Ge_{0.5}Si_{0.5})₂ with external pressure.

A. Magnetism and valence state of EuCu₂Ge₂ under high pressure

Figure 1(a) shows typical ME spectra of the antiferromagnetic EuCu₂Ge₂ sample ($T_N = 14$ K) collected at pressures up to 6.9 GPa at 4.2 K. All high-pressure ME spectra display a magnetic hyperfine splitting, indicating magnetic ordering of the Eu²⁺ ($4f^7$) moments at low temperature. These spectra, except the one at 6.9 GPa which will be discussed later, were fitted by a single component involving a magnetic hyperfine splitting. At higher temperatures $T = 120$ K in Fig. 1(b), no magnetic hyperfine splitting is observed, indicating a paramagnetic state prevails. Here the ME spectra were fitted by a single-site Lorentzian line with linewidth, isomer shift, and small quadrupole splitting as free parameters. The B_{eff} and isomer shift S parameters derived from the fitting in Fig. 1 as a function of pressure at 4.2 and 120 K are plotted in Figs. 2(a) and 2(b), respectively. All isomer shift values S are quoted relative to the SmF₃ source from here onwards. As is evident

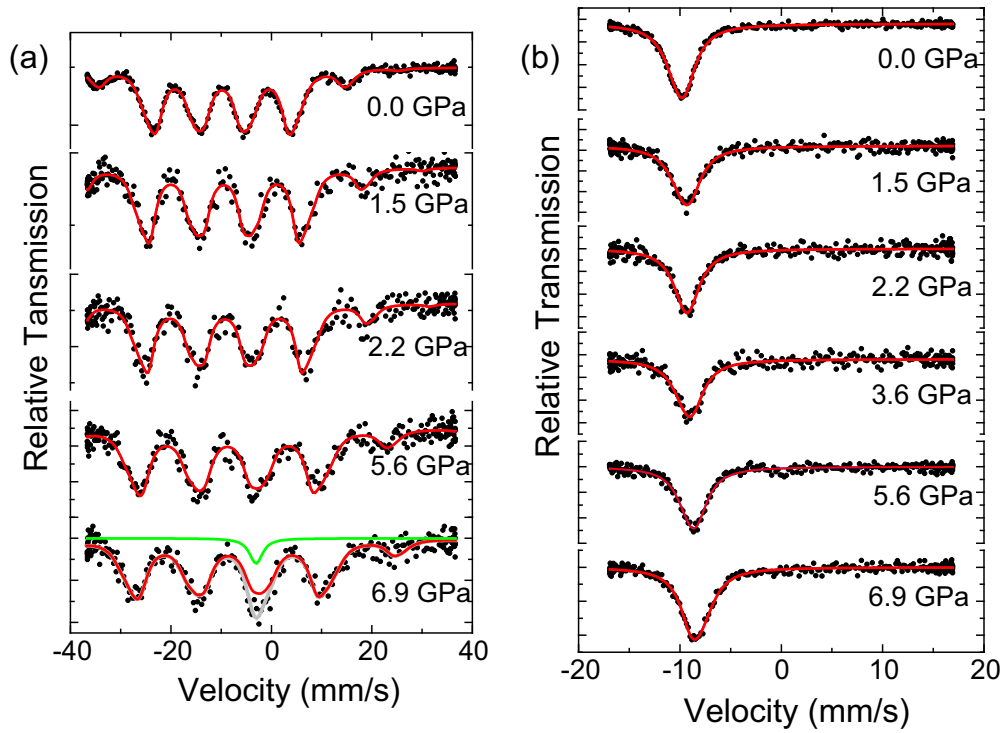


FIG. 1. ^{151}Eu Mössbauer spectra of EuCu_2Ge_2 at different pressures. (a) Spectra at 4.2 K. (b) Spectra at 120 K. Solid lines through the data points are the overall fit.

from Fig. 2(a), the magnitude of the magnetic hyperfine field increases nearly linearly with increasing pressure and $\partial B_{\text{eff}}/\partial P = 1.54 \text{ T GPa}^{-1}$.

To understand the origin of such an increase, we consider the contributions to B_{eff} . These can be mainly described in divalent Eu metallic systems as the sum of different contributions [26,36,37]:

$$B_{\text{eff}} = B_c + B_{ce} + B_{\text{thf}}. \quad (2)$$

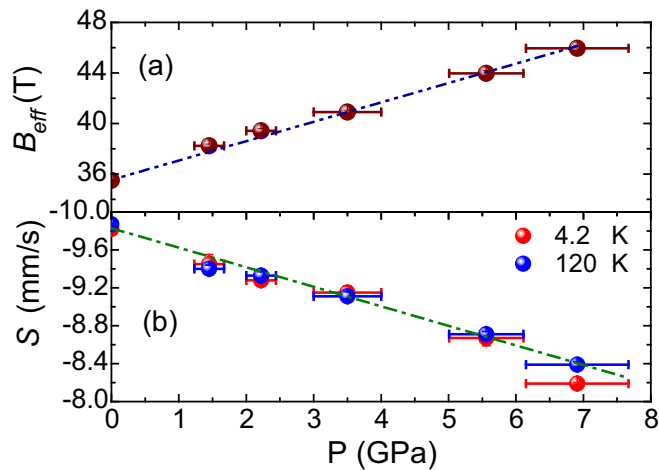


FIG. 2. (a) Magnetic hyperfine field behavior as a function of pressure in EuCu_2Ge_2 at 4.2 K. (b) Isomer shift S as a function of pressure at 4.2 and 120 K. Dashed line through the data points in both panels are to guide the eye.

B_c is the field (-34 T) from polarization of core s electrons by the $4f$ moment, B_{ce} arises from the conduction electron polarization by the Eu ion itself, and B_{thf} includes all transferred effects from $4f$ magnetic moments of neighboring magnetic ions that contribute to spin polarization of the conduction electrons. The observed increase of B_{eff} in EuCu_2Ge_2 with pressure is similar to that observed in stable divalent Eu compounds [37]; see also EuAu_2Si_2 [38] and EuAl_2 [39]. The increase of $|B_{\text{eff}}|$ with external pressure is mainly due to the increase of $|B_{\text{thf}}|$, caused by the enhancement of both intra-atomic and interatomic $4f$ ($5d$, $6s$) exchange interactions as reported in stable divalent Eu intermetallic compounds [37]. Thus, our high-pressure data clearly show that the magnetic moment of the Eu^{2+} state in EuCu_2Ge_2 is stable at pressures below 6.9 GPa. This is consistent with the observation of a weak pressure dependence of the isomer shift at 4.2 K as well as the absence of a temperature dependence in S between 4.2 and 120 K for pressures below 6.9 GPa [15], see Fig. 2(b).

Our finding that EuCu_2Ge_2 is in a stable Eu^{2+} valence state at ambient pressure and for higher pressures up to $\sim 6.9 \text{ GPa}$ is in agreement with those previously reported in Refs. [12–14] as well as with the high-pressure study of EuCu_2Ge_2 [21]. Our results are also in agreement with more recent angle-integrated photoemission spectroscopy and angle-resolved photoemission spectroscopy experiments using soft x rays on single crystals of EuCu_2Ge_2 [22].

This contradicts the suggestion from XANES measurements that EuCu_2Ge_2 exhibits an intermediate valence state already at ambient pressure [19,23,24].

Furthermore, at 6.9 GPa there is the appearance of a nonmagnetic single-line component with an isomer shift of $\sim -3.1 \text{ mm/s}$ superimposed on the magnetically split

spectrum with an isomer shift of ~ 8.53 mm/s [see Fig. 1(a)]. This indicates onset of a valence change of the Eu^{2+} state which is connected with a magnetic to nonmagnetic transition. We thus anticipate a pressure-induced quantum phase transition where a magnetic to nonmagnetic transition occurs together with a change of Eu^{2+} valence at pressures higher than ~ 7 GPa, beyond the capabilities of our large-volume pressure cell. Rather, such an interplay between valence and magnetic state changes in our accessible pressure range will be conspicuously demonstrated and discussed for the $x = 0.5$ composition of $\text{EuCu}_2(\text{Ge}_{1-x}\text{Si}_x)_2$ (Sec. III C).

B. Pressure-induced quantum phase transition in $\text{EuCu}_2(\text{Ge}_{1-x}\text{Si}_x)_2$, $x = 0.5$

The spectra of this composition at 300 and 4.2 K have identical isomer shifts at ambient pressure. Absence of any temperature-dependent isomer shift confirms this composition has an integral valence, Eu^{2+} , before pressurization [15,25].

Figure 3(a) displays the pressure dependence of the Mössbauer spectra collected at 4.2 K. In contrast to the case of EuCu_2Ge_2 in Fig. 1(a), any magnetic hyperfine splitting feature has completely disappeared at 3.6 GPa and a nonmagnetic state is prevalent up to 5.5 GPa. The onset of the magnetic to nonmagnetic transition is observed as low as 1.3 GPa [see Fig. 3(a)]. These spectra at and below 2.2 GPa could be adequately fitted by a superposition of nonmagnetic single-line and magnetically split spectral components.

The abundance of the non-magnetic component increases from $\sim 13\%$ at 1.3 GPa to $\sim 69\%$ at 2.2 GPa, at the expense of the magnetic component. This single-line component has an isomer shift $S \sim -3.5$ mm/s, intermediate to those of typical Eu^{2+} and Eu^{3+} integral valences which fall in the ranges $S_2 \sim -14$ to -8 mm/s and $S_3 \sim -1$ to $+4$ mm/s, respectively [15]. The disappearance of the magnetic component in Fig. 3(b) suggests that a first-order magnetic to nonmagnetic transition occurs at ~ 3.6 GPa. Additionally, the observation of two subspectra in a range beyond ambient pressure up to 3.6 GPa (see Fig. 3) implies: (i) existence of an inhomogeneous IV state, whose Eu mean valence state is determined by the weighted average isomer shift values of the two components and (ii) there is a pressure range spanning at least 1.3–2.2 GPa in which magnetic order and IV states coexist [40].

Upon disappearance of the magnetic component at ~ 3.6 GPa in Fig. 3, a second metastable IV component ($\sim 15\%$) at $S \sim -5.8$ mm/s coexists with the main IV component ($\sim 85\%$) at $S \sim -2.8$ mm/s that nucleated in the inhomogeneous IV regime at $P < 3.6$ GPa. This is depicted in the plot of relative abundances in Fig. 3(b), derived from spectral component area ratios. Further discussion on the coexisting IV components at 3.6 GPa is presented in the Supplemental Material [35]. For $P \geq 4.4$ GPa the metastable IV component disappears, resulting in a homogeneous IV state represented by a single-line component at $S \sim -2.5$ mm/s.

The pressure dependence of the parameters B_{eff} and S for the spectral components and the weighted average values are plotted in Figs. 4(a) and 4(b), respectively. For comparison the pressure dependences of B_{eff} and S of the electronically stable EuCu_2Ge_2 end-member reference is included in the plots. The

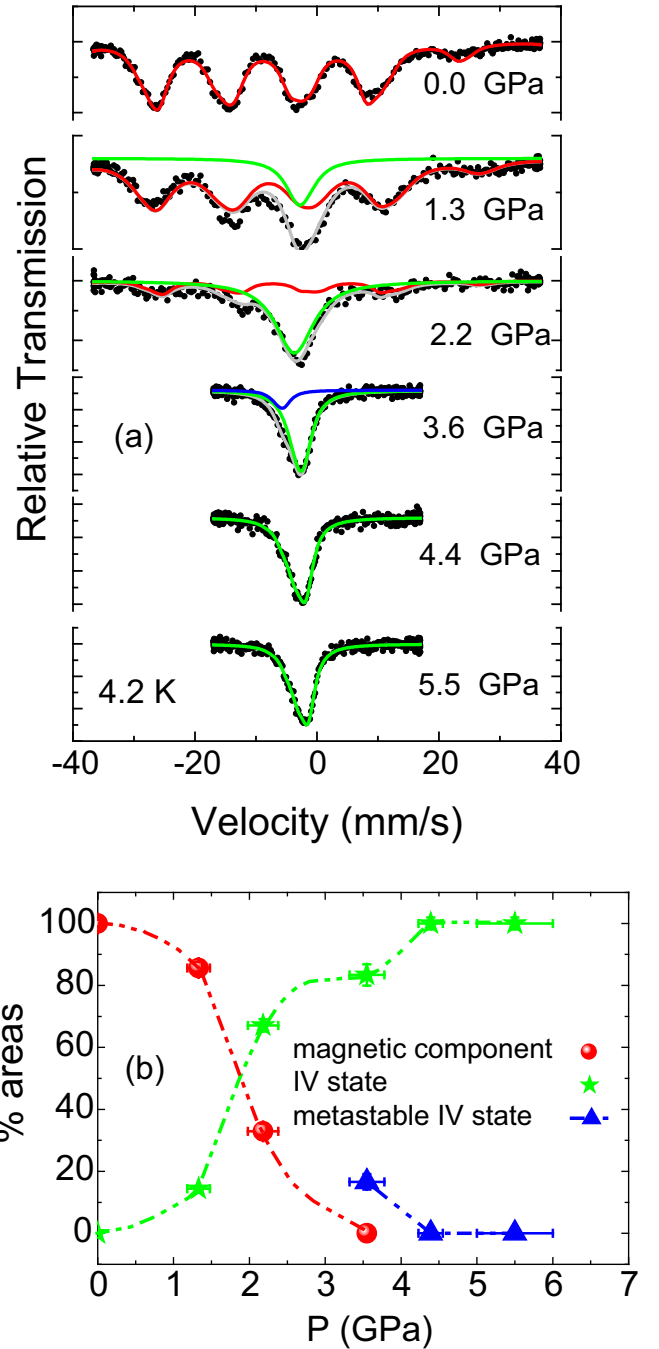


FIG. 3. (a) ^{151}Eu Mössbauer spectra at 4.2 K of $\text{EuCu}_2(\text{Ge}_{1-x}\text{Si}_x)_2$ for $x = 0.5$ at various pressures. Solid line through the data points is the overall fit. Two coexisting IV components at 3.6 GPa have been confirmed in a temperature-dependent study; see Sec. S2 of the Supplemental Material [35]. (b) Pressure dependence of the area ratio (abundances) of the spectral components in the Mössbauer spectra. Dashed lines through the data points are to guide the eye.

suppression of B_{eff} in Fig. 4(a) highlights the pressure-induced QPT for the sample with $x = 0.5$ at a QCP of $P_C \sim 3.6$ GPa. The comparatively strong pressure dependence of S for the $x = 0.5$ sample at 4.2 K in Fig. 4(b) is consistent with rapid collapse of magnetic order in Fig. 4(a) due to the suppression

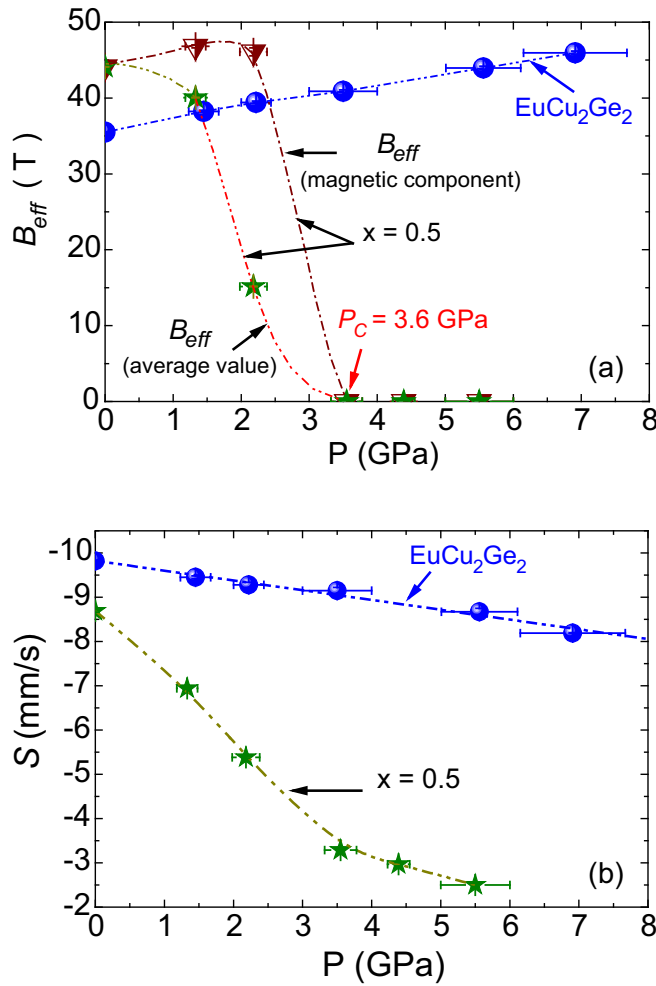


FIG. 4. (a) Effective magnetic hyperfine field (B_{eff}) as a function of pressure in $\text{EuCu}_2(\text{Ge}_{1-x}\text{Si}_x)_2$ for $x = 0$ and $x = 0.5$ at 4.2 K. (b) Isomer shift S as a function of pressure at 4.2 K. In the case of those spectra in the $x = 0.5$ composition which are comprised of two components with different isomer shifts, values of $S(P)$ are weighted average values of isomer shifts of the components. In both panels dashed lines through the data points are to guide the eye.

of the Eu $4f^7$ magnetic moment. The negative pressure dependence $\partial S/\partial P$ in Fig. 4(b) is particularly strong up to ~ 3 GPa, followed by much weaker pressure dependence. Figure 4 thus highlights the large pressure instigated deviations of the Eu valence from the divalent state that prevails at ambient pressure.

It is interesting to compare magnetic-electronic correlations in the two cases $x = 0$ and 0.5 of this pressure study. Pressure-induced changes of B_{eff} and S are plotted against each other for the two samples, as depicted in Fig. 5. For the electronically stable EuCu_2Ge_2 end member, both B_{eff} and S have positive pressure dependences, due to increasing intra- and interatomic $4f$ ($5d$, $6s$) exchange interactions expected in stable $4f$ moment systems [37–39]. Contrary to this $x = 0$ case the sample with $x = 0.5$, which undergoes pressure-induced collapse of magnetic order at ~ 3.6 GPa, exhibits a negative correlation between B_{eff} and S from the large negative pressure dependence of S in Fig. 4(b). Such a large change of isomer shift S is due to temporal fluctuations of a $4f$

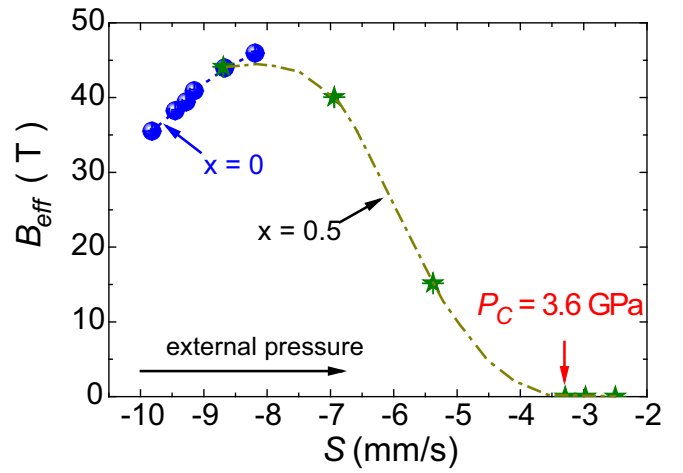


FIG. 5. Correlation between the magnetic hyperfine field (B_{eff}) and the isomer shift (S) in $\text{EuCu}_2(\text{Ge}_{1-x}\text{Si}_x)_2$ for $x = 0$ and $x = 0.5$ for different pressures at 4.2 K. Dashed lines through the data points are to guide the eye.

electron to the $5d$ conduction band ($4f^7 \Leftrightarrow 4f^6 + e^-$) and consequent breakdown of the $4f^7$ magnetic moment to render a nonmagnetic IV state. Estimations of the valence changes across the quantum phase transition with pressure will be discussed in the following section C.

We have then checked whether the observed pressure-induced quantum phase transition at ~ 3.6 GPa in the sample with $x = 0.5$ involves a structural phase transition. To this end we have measured the pressure dependence of the lattice parameters up to ~ 6 GPa at 300 K using energy-dispersive x-ray diffraction. Diffraction patterns at different pressures are shown in Fig. 6(a). All diffraction peaks could be identified with the tetragonal ThCr_2Si_2 -type structure, space group $I4/mmm$. Lattice parameters were determined from positions of the diffraction peaks at different pressures, using software described in the Experiment subsection II B. Errors of $\sim 0.5\%$ in the lattice parameters are mainly due to uncertainties in the positions of reflections. Values of the lattice parameters at ambient pressure are in good agreement with those of Hossain *et al.* [16]. The Birch-Murnaghan equation of state [41] has been fitted to the volume-pressure data in Fig. 6(b), to yield the isothermal bulk modulus $B_0 = 64 \pm 3$ GPa. This is insensitive as to whether the pressure derivative B'_0 is left as a free parameter or fixed at 4 as is often the case in such analysis. The pressure dependences of the lattice parameters and unit-cell volume are displayed in Fig. 6(b). These structural data indicate that to within the accuracy of our measurements, there is no evidence for a structural phase transition up to ~ 6 GPa. Nonlinear behavior of the increasing c/a ratio above 3 GPa is discerned and may be related to the change of valence and magnetic state at 3.6 GPa. Only high-resolution angle-resolved x-ray-diffraction experiments at low temperatures would provide better detail of any structural adjustments. Thus, the pressure-induced quantum phase transition in the $x = 0.5$ composition is not associated with a change of lattice symmetry, although there is hint of structural adjustments manifested in the pressure evolution of the c/a ratio. By comparison, there is no change of lattice symmetry

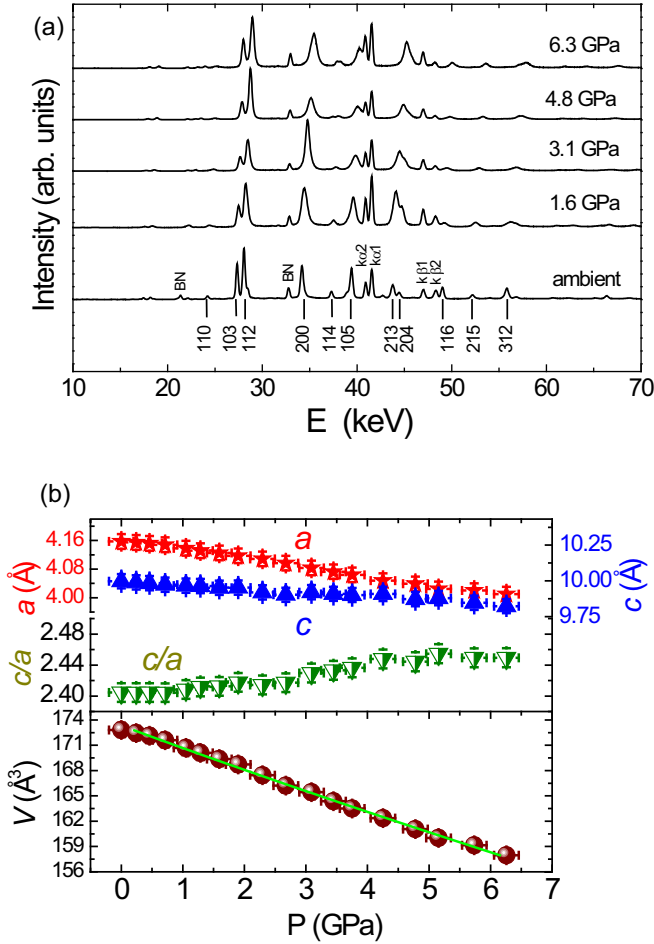


FIG. 6. (a) ED-XRD patterns at different pressures at 300 K for $\text{EuCu}_2(\text{Ge}_{1-x}\text{Si}_x)_2$, $x = 0.5$. (b) Lattice parameters a , c , ratio c/a , and unit-cell volume (V) as a function of pressure are in top and bottom panels, respectively. In the bottom panel the line through the measured data points (symbols) is a fit with the Birch-Murnaghan equation.

but there are anomalous changes of lattice parameters across the quantum phase transition induced by chemical substitution in the $\text{EuCu}_2(\text{Ge}_{1-x}\text{Si}_x)_2$ series [16].

C. Magnetism versus valence across the quantum phase transition

We now consider the mutual relationship between magnetic order and intermediate valence as the $x = 0.5$ composition is evolved through the pressure-induced quantum phase transition. In so doing a magnetic-electronic phase diagram is developed.

It is first necessary to calculate the pressure dependence of the Eu mean valence from S at 4.2 K (i.e., in the ground state). This is accomplished by using the data of Fig. 4(b) showing the pressure dependence of the isomer shift of both the stable EuCu_2Ge_2 and the sample with $x = 0.5$.

The pressure-induced change of the Eu isomer shift due to volume changes only is from a linear fit to the data for EuCu_2Ge_2 at 4.2 K, shown in Fig. 4(b). This corresponds to a negative slope of $\partial S_2/\partial P \sim 0.22 \text{ mm/s GPa}^{-1}$,

considered as a reference for the pressure dependence of electronic parameters of the stable Eu^{2+} valence state within the $\text{EuCu}_2(\text{Ge}_{1-x}\text{Si}_x)_2$ series.

The pressure-induced change of the valence from the divalent state $\nu(P) = 2 + \Delta\nu(P)$ at 4.2 K is obtained from the measured isomer shift at different pressures $S(P)$. In the framework of the interconfigurational fluctuation model [42,43], the relation between measured isomer shift at 4.2 K and change of valence $\Delta\nu(P)$ can be represented as follows [15,25,38]:

$$S(P) = S_2(P) + (S_3 - S_2)\Delta\nu(P), \quad (3)$$

where S_2 and S_3 are isomer shifts assigned to integral valence ions Eu^{2+} and Eu^{3+} at ambient pressure, respectively. The quantity $\Delta\nu(P)$ can also be considered as the occupation probability of the Eu^{3+} state. We have chosen S_2 to be -9.82 mm/s , the isomer shift of the stable Eu^{2+} state in EuCu_2Ge_2 ($x = 0$) and $S_3 = +0.44 \text{ mm/s}$ as the value of the stable Eu^{3+} state of EuFe_2Si_2 which also crystallizes in the tetragonal ThCr_2Si_2 -type structure [25]. Thus $S_3 - S_2 = 10.26 \text{ mm/s}$. For $S_2(P)$ we have used the slope of the linear fit to the data of EuCu_2Ge_2 in Fig. 4(b). We suppose this determines the pressure dependence of the Eu^{2+} isomer shift associated with the lattice deformation of the $x = 0.5$ composition. In the case of a spectrum comprising two components with different isomer shifts (see Fig. 3), values of $S(P)$ are weighted average values which correspond to the Eu mean valence at a particular pressure.

The results of our evaluation of $\nu = 2 + \Delta\nu(P)$ from $S(P)$ in Fig. 4(b) enable us to develop the phase diagram in Fig. 7(a). This captures the change of both the valence and magnetic ground states across the pressure-induced quantum phase transition. The main features in the phase diagram are (i) the original Eu^{2+} AF state first collapses into a mixed state extending up to some pressure in the range 2.2–3.6 GPa involving an inhomogeneous IV state coexisting with a magnetically ordered state, (ii) at higher pressures above the QCP at ~ 3.6 GPa, the system undergoes crossover to a nonmagnetic homogeneous IV state at $P \geq 4.4$ GPa, exemplified in the ME spectra in Fig. 3(a), and (iii) the high value of $\nu \sim 2.5$ attained in the IV state at $P_C \sim 3.6$ GPa reflects enhanced charge fluctuations at the QCP.

The enhanced charge fluctuations occurring at the QCP remain nearly constant up to 5.5 GPa. Thus we speculate that such enhanced charge fluctuations at and beyond the QCP may lead to the formation of an unusual ground state as has been suggested recently to explain the superconductivity in CeCu_2Si_2 [8,9]. We have checked for superconductivity at or near the pressure-induced QCP of $\text{EuCu}_2(\text{Ge}_{0.5}\text{Si}_{0.5})_2$ in resistance-temperature scans under hydrostatic pressure up to ~ 3 GPa at low temperatures down to 40 mK. Figure 7(b) displays the pressure dependence of $T_N(P)$ as deduced from signatures in the temperature dependence of the resistance at different pressures [35]. $T_N(P)$ behaves in a similar way to the weighted average $B_{\text{eff}}(P)$ in Fig. 7(a) and collapses near the QCP. As is evident from the inset of Fig. 7(b), we find no evidence for superconductivity down to 40 mK.

The absence of superconductivity at the pressure-induced QCP of $\text{EuCu}_2(\text{Ge}_{0.5}\text{Si}_{0.5})_2$ where Eu valence fluctuations are enhanced, is not in accord with the suggestion that

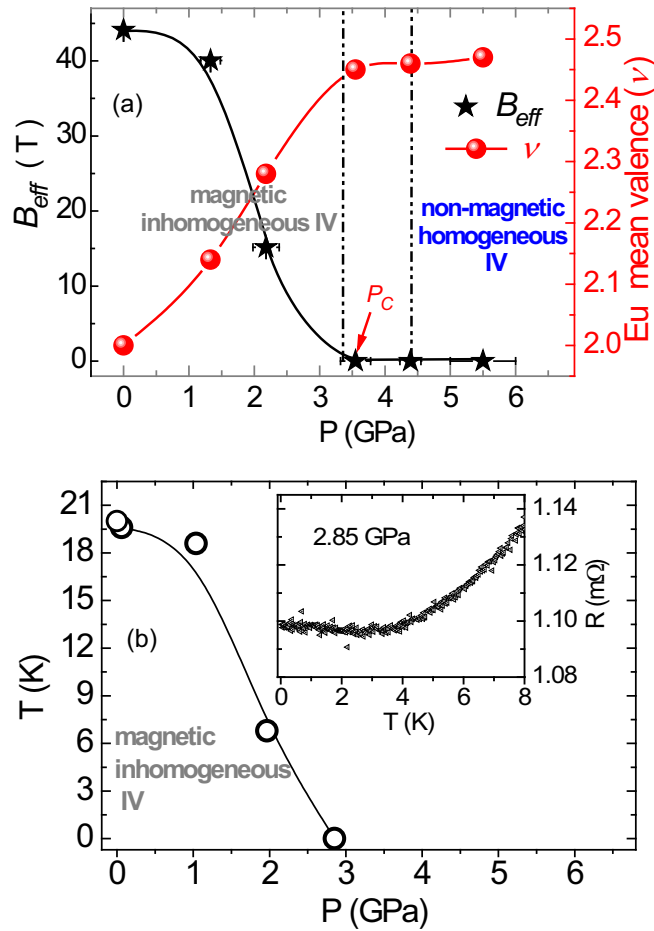


FIG. 7. (a) Phase diagram of $\text{EuCu}_2(\text{Ge}_{1-x}\text{Si}_x)_2$ for $x = 0.5$ at 4.2 K, indicating the change of magnetic ground state and valence state across the pressure-induced QPT. Eu mean valence is obtained from the measured isomer shift at 4.2 K in Fig. 4(b) and Eq. (3). See Sec. III C of the text. $B_{\text{eff}}(T)$ are the weighted average values from subcomponents in the spectrum [Figs. 3(b) and 4(a)]. Solid lines through the data points are to guide the eye. (b) T_N as a function of pressure up to the vicinity of the QCP at 3.6 GPa. Line through the data symbols is to guide the eye. Inset shows the temperature dependence of the resistance down to 40 mK at the ~ 2.85 -GPa onset of the maximum in valence fluctuations $\nu \sim 2.45$.

superconductivity observed in CeCu_2Si_2 at a QCP near 4 GPa is linked to valence fluctuations. That IV regime in CeCu_2Si_2 is decoupled from the magnetic fluctuations regime at ambient pressure where superconductivity also occurs [8,9]. By contrast $\text{EuCu}_2(\text{Ge}_{0.5}\text{Si}_{0.5})_2$ is a case where valence fluctuations are intimately coupled to the collapse of magnetism and at the magnetic QCP both charge and spin fluctuations exist. This hinders a direct comparison between the two systems.

IV. SUMMARY CONCLUSIONS

The series $\text{EuCu}_2(\text{Ge}_{1-x}\text{Si}_x)_2$ combines the divalent Eu antiferromagnetic compound EuCu_2Ge_2 with the nonmagnetic IV compound EuCu_2Si_2 . Our ^{151}Eu ME probe of $x = 0$ and $x = 0.5$ fixed compositions while varying pressure, lends microscopic insight into the ground-state properties of the system and the interplay between changes in magnetism and valence state, in particular pressure tuning across a QCP involving valence fluctuations. These compositions have been pressurized from ambient pressure to 7 GPa, including variable temperature scans in the range 300–4.2 K.

In the end-member EuCu_2Ge_2 , both the magnetic and divalent Eu states are found to be stable up to ~ 7 GPa. This then constitutes a reference system for the $x = 0.5$ composition, which undergoes collapse of magnetic ordering initiated at ~ 1.3 GPa. Up to at least 2.2 GPa there is an associated large shift of the Eu mean valence from the initial divalent state. This manifests as a mixed state in which an inhomogeneous IV state coexists with a magnetically ordered state. The ^{151}Eu ME probe shows that this mixed state precedes the pressure-induced QPT to a nonmagnetic homogeneous IV state occurring beyond a critical pressure of 3.6 GPa, suggesting that a first-order phase transition occurs. The ThCr_2Si_2 -type lattice structure remains unchanged upon evolving the sample through the QCP identified at ~ 3.6 GPa. In addition, the Eu mean valence attains its largest value $\nu \sim 2.45$ at the QCP and plateaus thereafter, indicating enhanced charge fluctuations ($4f^7 \Leftrightarrow 4f^6 + e^-$) occur in the vicinity of the QCP. High-pressure resistivity measurements at low temperatures down to 40 mK near the QCP show no indication of superconductivity. A corresponding phase diagram has been constructed from these results of the $x = 0.5$ composition involving the QCP at ~ 3.6 GPa.

These results will potentially contribute to and enhance our understanding of the interplay between valence fluctuations and unusual ground states in strongly correlated $4f$ systems evolved through a QPT. It is also of interest to similarly deploy the variable-temperature ^{151}Eu microscopic probe of Eu mean valence in the $\text{EuCu}_2(\text{Ge}_{1-x}\text{Si}_x)_2$ series as composition is evolved through the QCP at $x \sim 0.7$, for comparison with the pressure-induced quantum phase transition of the $x = 0.5$ composition investigated in our study.

ACKNOWLEDGMENTS

Resistance-temperature measurements at high pressure were performed in the Materials Growth and Measurement Laboratory MGML (www.mgml.eu), which is supported within the program of Czech Research Infrastructures (Project No. LM2018096). G.R.H. acknowledges financial support from the National Research Foundation of South Africa (Grant No. 105870).

- [1] M. Vojta, Quantum phase transitions, *Rep. Prog. Phys.* **66**, 2069 (2003).
 [2] C. Pfleiderer, D. Reznik, L. Pintschovius, H. v. Löhneysen, M. Garst, and A. Rosch, Partial order in the non-

- Fermi-liquid phase of MnSi, *Nature (London)* **427**, 227 (2004).
 [3] N. D. Mathur, F. M. Grosche, S. R. Julian, I. R. Walker, D. M. Freye, R. K. W. Haselwimmer, and G. G. Lonzarich,

- Magnetically mediated superconductivity in heavy fermion compounds, *Nature (London)* **394**, 39 (1998).
- [4] S. Saxena, P. Agarwal, K. Ahilan, F. Grosche, R. Haselwimmer, M. Steiner, E. Pugh, I. Walker, S. Julian, and P. Monthoux, Superconductivity on the border of itinerant-electron ferromagnetism in UGe_2 , *Nature (London)* **406**, 587 (2000).
- [5] B. Bogenberger and H. v. Löhneysen, Tuning of non-Fermi-Liquid Behavior with Pressure. *Phys. Rev. Lett.* **74**, 1016 (1995).
- [6] F. Grosche, S. Julian, N. Mathur, and G. Lonzarich, Magnetic and superconducting phases of CePd_2Si_2 , *Phys. B: Condens. Matter* **223**, 50 (1996).
- [7] I. Walker, F. Grosche, D. Freye, and G. Lonzarich, The normal and superconducting states of CeIn_3 near the border of antiferromagnetic order, *Phys. C: Superconductivity* **282**, 303 (1997).
- [8] H. Yuan, F. Grosche, M. Deppe, C. Geibel, G. Sparn, and F. Steglich, Observation of two distinct superconducting phases in CeCu_2Si_2 , *Science* **302**, 2104 (2003).
- [9] A. T. Holmes, D. Jaccard, and K. Miyake, Signatures of valence fluctuations in CeCu_2Si_2 under high pressure, *Phys. Rev. B*, **69**, 024508 (2004).
- [10] M. Debessai, T. Matsuoka, J. Hamlin, J. Schilling, and K. Shimizu, Pressure-Induced Superconducting State of Europium Metal at Low Temperatures. *Phys. Rev. Lett.* **102**, 197002 (2009).
- [11] W. Bi, J. Lim, G. Fabbris, J. Zhao, D. Haskel, E. E. Alp, M. Y. Hu, P. Chow, Y. Xiao, and W. Xu *et al.*, Magnetism of europium under extreme pressures, *Phys. Rev. B* **93**, 184424 (2016).
- [12] I. Felner and I. Nowik, Magnetism and hyperfine interactions in EuM_2Ge_2 and GdM_2Ge_2 ($M = \text{Mn, Fe, Co, Ni, Cu}$), *J. Phys. Chem. Solids* **39**, 767 (1978).
- [13] P. Wang, Z. Stadnik, J. Zukrowski, B. Cho, and J. Kim, Magnetic properties and hyperfine interactions in EuCu_2Ge_2 single crystals, *Solid State Commun.* **150**, 2168 (2010).
- [14] W. N. Rowan-Weetaluktuk, D. H. Ryan, P. Lemoine, and J. M. Cadogan, Thermal neutron diffraction determination of the magnetic structure of EuCu_2Ge_2 , *J. Appl. Phys.* **115**, 17E101 (2014).
- [15] E. Bauminger, D. Froindlich, I. Nowik, S. Ofer, I. Felner, and I. Mayer, Charge Fluctuations in Europium in Metallic EuCu_2Si_2 , *Phys. Rev. Lett.* **30**, 1053 (1973).
- [16] Z. Hossain, C. Geibel, N. Senthilkumaran, M. Deppe, M. Baenitz, F. Schiller, and S. Molodtsov, Antiferromagnetism, valence fluctuation, and heavy-fermion behavior in $\text{EuCu}_2(\text{Ge}_{1-x}\text{Si}_x)_2$, *Phys. Rev. B* **69**, 014422 (2004).
- [17] S. Fukuda, Y. Nakanuma, J. Sakurai, A. Mitsuda, Y. Isikawa, F. Ishikawa, T. Goto, and T. Yamamoto, Application of Doniach diagram on valence transition in $\text{EuCu}_2(\text{Si}_x\text{Ge}_{1-x})_2$, *J. Phys. Soc. Jpn.* **72**, 3189 (2003).
- [18] P. Alekseev, K. Nemkovski, J. Mignot, V. Lazukov, A. Nikonov, A. Menushenkov, A. Yaroslavtsev, R. Bewley, J. Stewart, and A. Griбанov, Magnetic excitations in $\text{EuCu}_2(\text{Si}_x\text{Ge}_{1-x})_2$: From mixed valence towards magnetism, *J. Phys.: Condens. Matter* **24**, 375601 (2012).
- [19] P. A. Alekseev, K. Nemkovski, D. Kozlenko, A. P. Menushenkov, A. Yaroslavtsev, A. Griбанov, E. Clementyev, C. Pantalei, B. Klobes, and R. Hermann, Coexistence of long range magnetic order and intervalent state of Eu in $\text{EuCu}_2(\text{Si}_x\text{Ge}_{1-x})_2$: Evidence from neutron diffraction and spectroscopic studies, *JETP Lett.* **99**, 164 (2014).
- [20] S. Doniach, The Kondo lattice and weak antiferromagnetism, *Physica B+C* **91**, 231 (1977).
- [21] W. Iha, T. Yara, Y. Ashitomi, M. Kakihana, T. Takeuchi, F. Honda, A. Nakamura, D. Aoki, J. Gouchi, and Y. Uwatoko, Electronic states in $\text{EuCu}_2(\text{Ge}_{1-x}\text{Si}_x)_2$ based on the Doniach phase diagram, *J. Phys. Soc. Jpn.* **87**, 064706 (2018).
- [22] I. Kawasaki, S.-i. Fujimori, Y. Takeda, H. Yamagami, W. Iha, M. Hedo, T. Nakama, and Y. Ōnuki, Electronic states of EuCu_2Ge_2 and EuCu_2Si_2 studied by soft x-ray photoemission spectroscopy, *Phys. Rev. B* **100**, 035111 (2019).
- [23] A. Geondzhian, A. Yaroslavtsev, P. Alekseev, R. Chernikov, B. Gaynanov, F. Baudalet, L. Nataf, and A. Menushenkov, Pressure-induced electronic phase transition in compound EuCu_2Ge_2 , *J. Phys.: Conf. Ser.* **712**, 012112 (2016).
- [24] K. S. Nemkovski, D. P. Kozlenko, P. A. Alekseev, J.-M. Mignot, A. P. Menushenkov, A. A. Yaroslavtsev, E. S. Clementyev, A. S. Ivanov, S. Rols, and B. Klobes, Europium mixed-valence, long-range magnetic order, and dynamic magnetic response in $\text{EuCu}_2(\text{Si}_x\text{Ge}_{1-x})_2$, *Phys. Rev. B* **94**, 195101 (2016).
- [25] I. Nowik, Mössbauer studies of valence fluctuations, *Hyperfine Interact.* **13**, 89 (1983) and references therein.
- [26] U. F. Klein, G. Wortmann, and G. Kalvius, High-pressure Mössbauer study of hyperfine interactions in magnetically ordered europium chalcogenides: EuO , EuS , EuTe , *J. Magn. Magn. Mater.* **3**, 50 (1976).
- [27] J. S. Schilling, U. F. Klein, and W. B. Holzapfel, Versatile high pressure cell for use at low temperatures, *Rev. Sci. Instrum.* **45**, 1353 (1974).
- [28] B. Bireckoven and J. Wittig, A diamond anvil cell for the investigation of superconductivity under pressures of up to 50 GPa: Pb as a low temperature manometer, *J. Phys. E: Sci. Instrum.* **21**, 841 (1988).
- [29] Written by R. A. Brand, Universität-GH-Duisburg and distributed by Wissel GmbH (D-82319 Starnberg, Germany). See <http://www.wissel-instruments.de>.
- [30] O. Shimomura, S. Yamaoka, T. Yagi, M. Wakatsuki, K. Tsuji, O. Fukunaga, H. Kawamura, K. Aoki, and S. Akimoto, Recent Advance with Anvil Devices, in *Solid State Physics under Pressure*, edited by S. Minomura (KTK/Reidel, Tokyo/Dordrecht, 1985), p. 351.
- [31] D. L. Decker, High-pressure equation of state for NaCl , KCl , and CsCl , *J. Appl. Phys.* **42**, 3239 (1971).
- [32] N. Fujiwara, T. Matsumoto, K. Koyama-Nakazawa, A. Hisada, and Y. Uwatoko, Fabrication and efficiency evaluation of a hybrid NiCrAl pressure cell up to 4 GPa, *Rev. Sci. Instrum.* **78**, 073905 (2007).
- [33] K. Murata, H. Yoshino, H. O. Yadav, Y. Honda, and N. Shirakawa, Pt resistor thermometry and pressure calibration in a clamped pressure cell with the medium, Daphne 7373, *Rev. Sci. Instrum.* **68**, 2490 (1997).
- [34] K. Yokogawa, K. Murata, H. Yoshino, and S. Aoyama, Solidification of high-pressure medium Daphne 7373, *Jpn. J. Appl. Phys.* **46**, 3636 (2007).
- [35] See Supplemental Material at <http://link.aps.org/supplemental/10.1103/PhysRevB.101.205127>, which includes resistance-temperature scans at various pressures and discussion of the temperature dependence of the intermediate valence behavior in the vicinity of the QCP at ~ 3.6 GPa.

- [36] I. Nowik, B. Dunlap, and J. Wernick, Contributions to the hyperfine field in europium intermetallics, *Phys. Rev. B* **8**, 238 (1973).
- [37] M. Abd-Elmeguid, H. Micklitz, and G. Kaindl, Volume dependence of magnetic hyperfine fields in Eu-intermetallic compounds, *Phys. Rev. B* **23**, 75 (1981).
- [38] M. Abd-Elmeguid, C. Sauer, and W. Zinn, Pressure-Induced Valence Change of Eu in $\text{Eu}(\text{Pd}_{0.8}\text{Au}_{0.2})_2\text{Si}_2$: Collapse of Magnetic Order, *Phys. Rev. Lett.* **55**, 2467 (1985).
- [39] A. Gleissner, W. Potzel, J. Moser, and G. M. Kalvius, EuAl_2 at Pressures up to 41 GPa: A Localized Magnet Exhibiting Highly Nonlinear Electronic Effects, *Phys. Rev. Lett.* **70**, 2032 (1993).
- [40] In this mixed-state regime there are regions of the sample that exhibit magnetic ordering involving Eu^{2+} valence states, coexisting with regions in which Eu is in an IV state. Pressurization at constant $T = 4.2$ K drives a change in relative populations of these coexisting states, where the state with a smaller atomic volume (higher valence) is energetically favored with increasing pressure. See also Sec. S2 of the Supplemental Material.
- [41] F. Birch, Finite strain isotherm and velocities for single-crystal and polycrystalline NaCl at high-pressures and 300 K, *J. Geophys. Res.* **83**, 1257 (1978).
- [42] D. Wohlleben, in *Valence Fluctuations in Solids*, edited by L. M. Falicov, W. Hanke, and M. B. Maple (North-Holland, Amsterdam, 1981), p. 1.
- [43] J. Röhler, D. Wohlleben, G. Kaindl, and H. Balster, Energy Balance of Mixed-Valent Eu Ions, *Phys. Rev. Lett.* **49**, 65 (1982).